NAVY DEPARTMENT
BUREAU OF ORDNANCE
CONTRACT NORD 9612

# HYDRODYNAMIC CHARACTERISTICS OF THE 500 POUND T16 S.P. BOMB



HYDRODYNAMICS LABORATORY
CALIFORNIA INSTITUTE OF TECHNOLOGY
PASADENA, CALIFORNIA

LABORATORY REPORT NO. N-51

COPY NO. 92

NAVY DEPARTMENT
BUREAU OF ORDNANCE
CONTRACT NOrd 9612

# HYDRODYNAMIC CHARACTERISTICS OF THE 500 POUND T16 S. P. BOMB

ROBERT T. KNAPP
DIRECTOR

HYDRODYNAMICS LABORATORY
CALIFORNIA INSTITUTE OF TECHNOLOGY
PASADENA, CALIFORNIA

Laboratory Report No. N-51

February 14, 1947

Report Prepared by
Gerald B. Robison
Hydraulic Engineer

# TABLE OF CONTENTS

## Summary

Reported herein are tests of the 500 pound T 16 S.P. Bomb covering the hydrodynamic force coefficients with and without cavitation, incipient cavitation characteristics, and flow lines as revealed in the Polarized Light Flume. It was not possible to cause full cavitation with present water tunnel limitations.

For noncavitating conditions, values were as follows:

| | Force Coefficient | Yaw $0^\circ$ | Yaw $10^\circ$ | Pitch $0^\circ$ | Pitch $10^\circ$ |
|---|---|---|---|---|---|
| Air-flight | $C_D$ | 0.215 | 0.355 | 0.228 | 0.375 up<br>0.325 down |
| | $C_C, C_L$ | 0 | 0.93 | 0 | 0.85 up<br>0.99 down |
| | $C_M$ | 0 | −0.176 | +0.006 | −0.197 up<br>+0.238 down |
| Water-flight | $C_D$ | 0.285 | 0.420 | 0.298 | 0.405 |
| | $C_C, C_L$ | 0 | 0.325 | 0 | 0.280 up<br>0.250 down |
| | $C_M$ | 0 | +0.085 | +0.006<br>−0.006 | +0.091 up<br>−0.079 down |

For maximum cavitation obtained, $C_D$ varied from 0.375 at $0^\circ$ to 0.385 at $4^\circ$. At $4^\circ$ also, $C_C$ was 0.19 and $C_M$, + 0.038.

Steady incipient cavitation was as follows:

| Location | K |
|---|---|
| Forward lug | 2.09 |
| Forward edge lug support | 1.92 |
| After lug | 1.65 |
| Nose | 1.41 |
| Lead edge of fins | 1.02 |
| Tail struts | 0.81 |
| Junction of afterbody | 0.56 |
| Junction of nose | 0.54 |

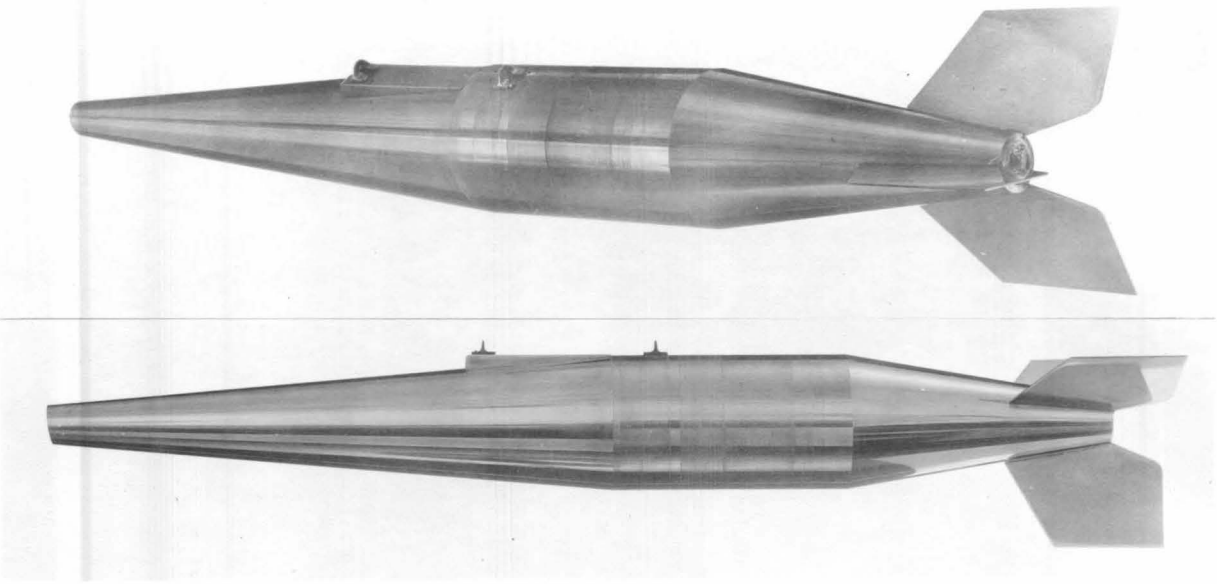

FIG. 1 – AIR–FLIGHT MODEL OF 500 LB T16 S.P. BOMB

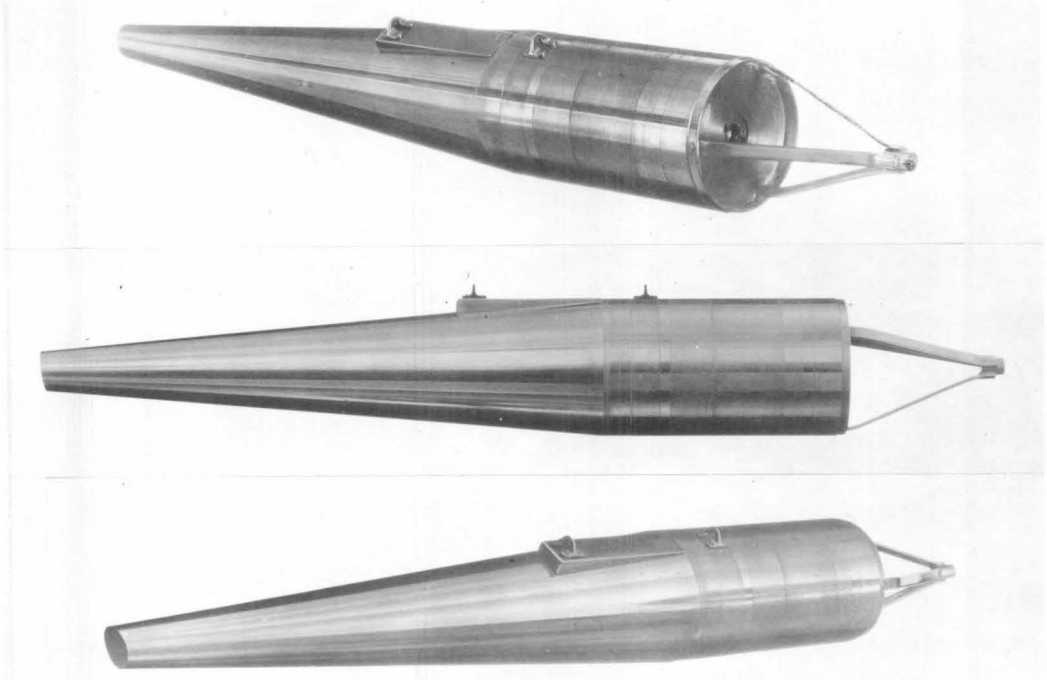

FIG. 2 – WATER–FLIGHT MODEL OF 500 LB T16 S.P. BOMB

# HYDRODYNAMIC CHARACTERISTICS OF THE 500-POUND T16 S.P. BOMB

## GENERAL

The tests reported herein were requested by Vice Admiral G. F. Hussey, Jr. in a letter to Dr. Knapp dated 13 May 1946. The work was performed under Contract NOrd 9612 in the Hydrodynamics Laboratory at the California Institute of Technology.

## PURPOSE

The purpose of the tests was to obtain the hydrodynamic force coefficients, both without cavitation and in a full cavitation bubble; to determine incipient cavitation characteristics; and to study the flow around the projectile in the Polarized Light Flume.

## PHYSICAL DATA

The prototype is described as a 500-pound version of an experimental bomb developed by German investigation and modified by the Bureau of Ordnance, Navy Department. It is intended for release at speeds of approximately 600 knots at low entry angles. For the air-flight portion of its trajectory, there is a conical afterbody with a three-vane tail which breaks away from the bomb on entry, leaving only internal tail structure. Figure 1 shows two views of the air-flight model, and Figure 2 shows three views of the water-flight model.

Prototype Dimensions

| | |
|---|---|
| Over-all length, air-flight | 94.45 inches |
| Distance from nose to approximate C.G. | 42.95 " |
| Maximum diameter | 11.80 " |
| Area of maximum cross section | 109.36 sq. in. |
| Total weight | 465.24 lbs. |

Model Dimensions

| | |
|---|---|
| Diameter | 2.000 inches |
| Over-all length, air-flight | 16.008 " |
| Distance, nose to C.G. | 7.28 " |
| nose to support point | 8.517 " |
| Scale ratio | 1 to 5.90 |

All parts of these models, except cylindrical body sections, were constructed and furnished by the Bureau of Ordnance.

Figure 3 is an outline drawing showing the air-flight model and the water-flight afterbody.

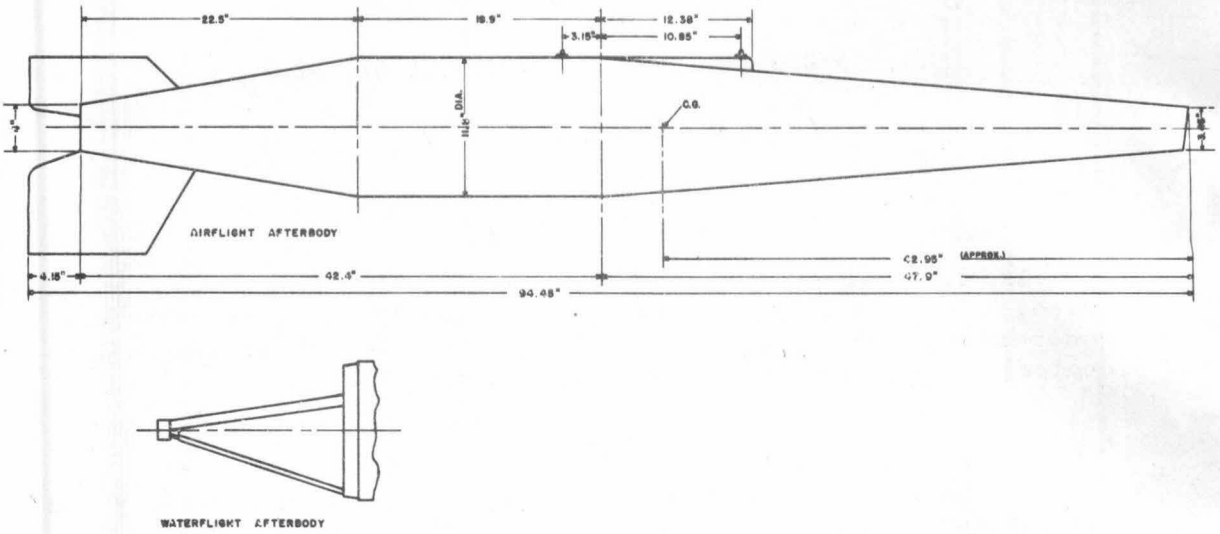





FIG. 3 – OUTLINE OF 500 LB T16 S.P. BOMB

## TEST CONDITIONS AND RESULTS

### Noncavitation Force Coefficients

This projectile is symmetrical about the vertical plane through its longitudinal axis, but asymmetrical about the horizontal plane at the nose tip, lugs, lug platform, and fins. This horizontal asymmetry causes a moment in the vertical plane which registers as an additional drag force on the three-component balance system used in the Water Tunnel. It thus became necessary to measure the drag in the normal upright position, that is, at 0-degree index and again, when rotated 180 degrees around its longitudinal axis. In the 180-degree position, the moment in the vertical plane reverses direction and the registered drag is less by the amount it was greater in the 0-degree position. The true drag is the average of corresponding readings. The asymmetry also makes a difference in the drag encountered with yawing and with pitching. Drag due to pitch angle was obtained by yawing the model when mounted at a 90-degree index.

The yaw and pitch tests were made with a velocity of 32 feet per second. All force coefficients were corrected for shield interference and the drag coefficient was also corrected for horizontal buoyancy.

Figure 4 shows the influence of yaw and pitch angles, to $\pm$ 10 degrees, upon the drag coefficient $C_D$, for both air-flight and water-flight models. The top left plot is for the air-flight model when yawed. The solid lines are for the normal and 180-degree index positions, given for their possible usefulness. The dash line is the desired average. The crossing of the two solid lines appears to be due to the effect of the air-flight afterbody and fins as no intersection occurs for similar curves with the water-flight afterbody. The lower left plot shows the effect of pitch

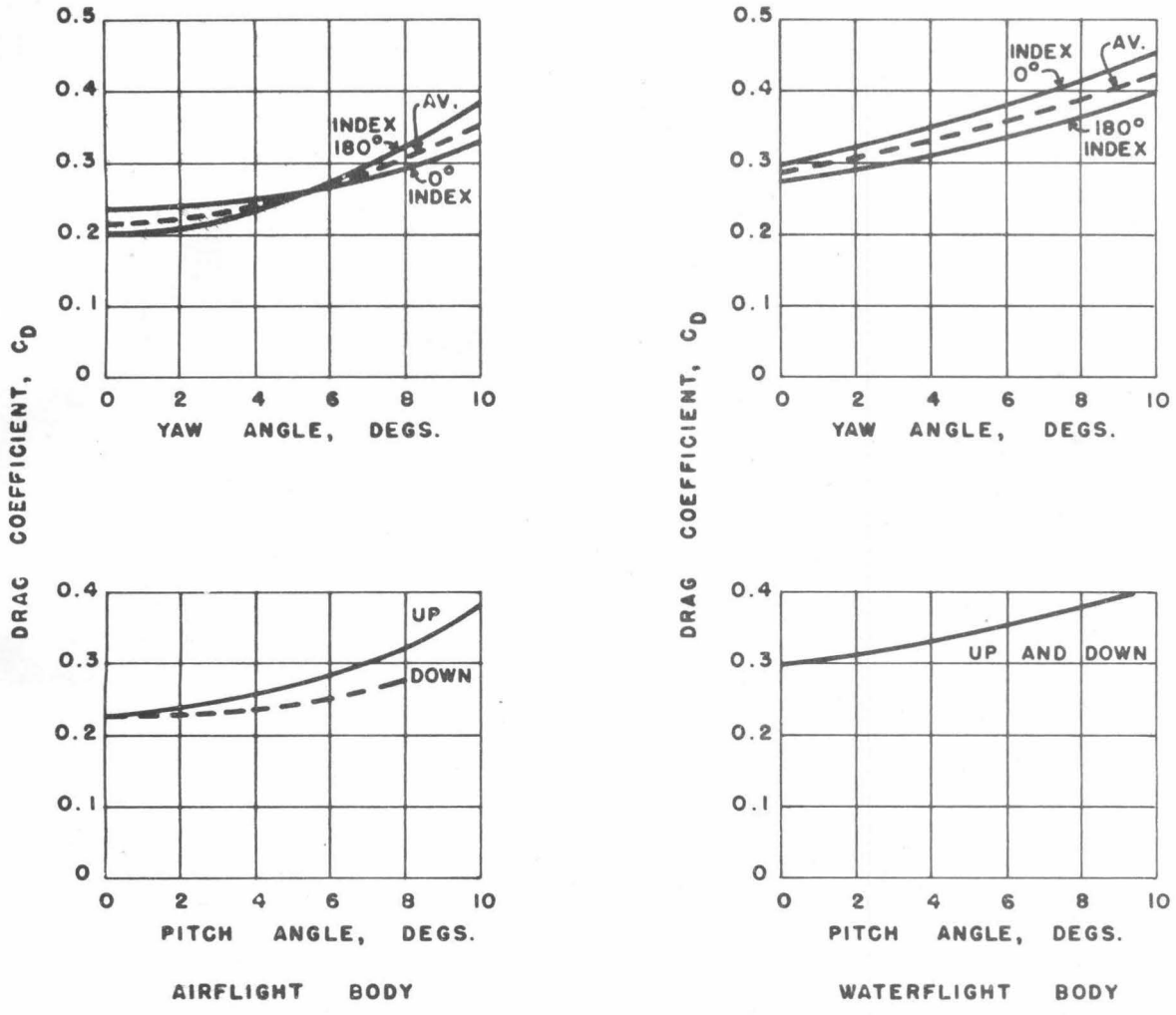


FIG. 4 — INFLUENCE OF YAW AND PITCH ANGLES ON DRAG COEFFICIENT FOR 500 LB T16 S.P. BOMB

on the drag coefficient of the air-flight model. The divergence for up and down pitch again seems to be due to the afterbody and fins. It may be noted that the average curve of the first plot is between the two branches for pitch angles, except below 2 degrees when the average curve is slightly lower. The plots on the right half of Figure 4 are for the water-flight model, the top one being for yaw and the bottom one for pitch angle variation. In both cases $C_D$ values are higher than for the air-flight model because of the additional form drag of the abrupt afterbody. In all plots of this figure, $C_D$ values are, of course, positive for both plus and minus yaw or pitch angles. The unusual shape of this projectile made unavoidable a support point considerably aft of the center of gravity, the point ordinarily chosen. Expressed in percentage of the total length, the center of gravity was 45.5 per cent (aft of the nose tip). The support points of the air-flight and water-flight models, while the same linear distance from the

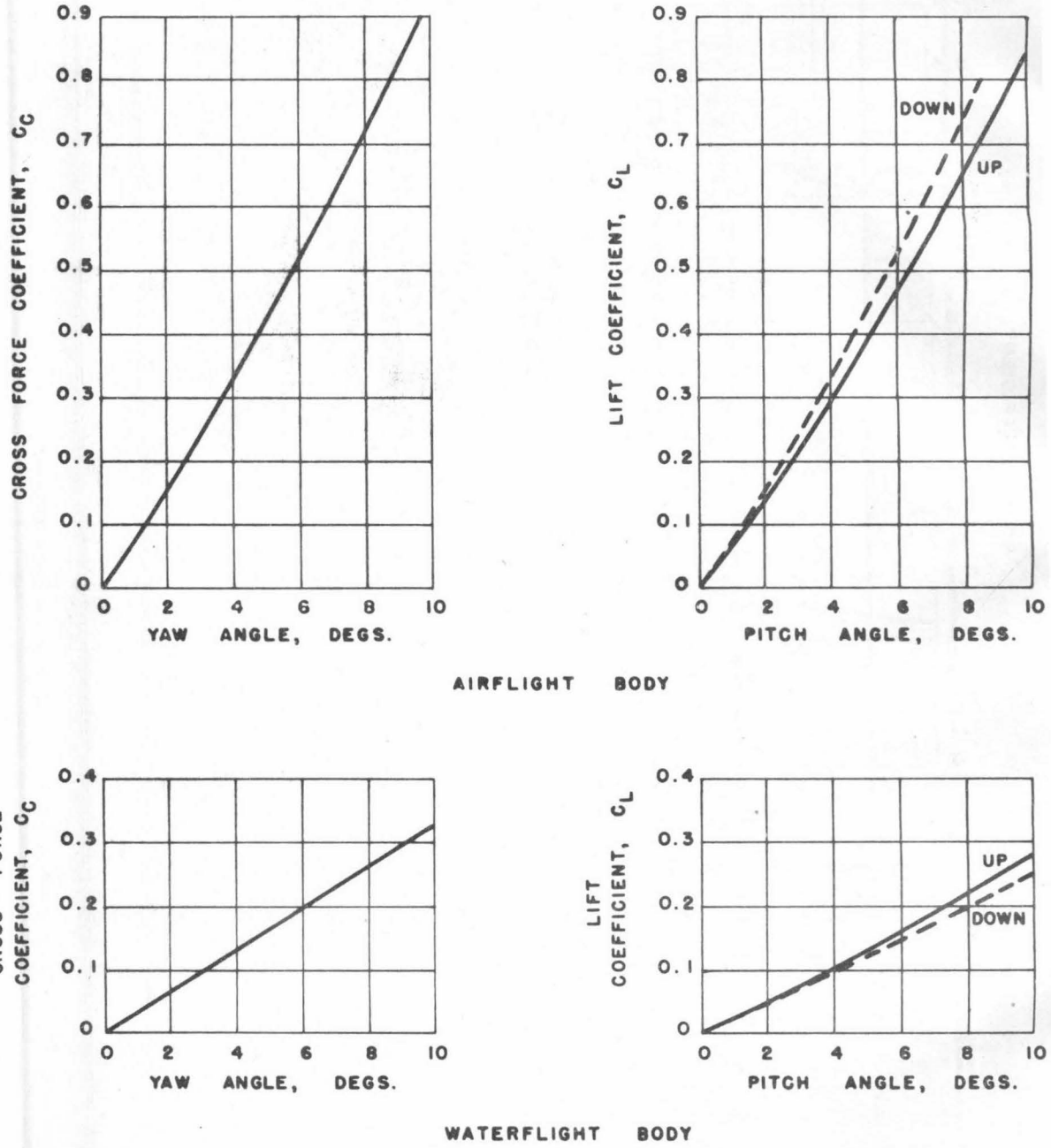


FIG. 5 — INFLUENCE OF YAW AND PITCH ANGLES ON CROSS FORCE AND LIFT COEFFICIENTS FOR 500 LB T16 S.P. BOMB

nose tip, were 53 per cent and 61 per cent of the respective overall lengths. Tests of the influence of support point on readings indicate that the drag coefficient values shown are likely to be higher by about 8 per cent and 13 per cent for the air- and waterflight bodies, respectively, as compared to test results with a support at the center of gravity.

Figure 5 indicates the variation of the cross force coefficient, $C_{\Sigma}$, with yaw and the lift coefficient, $C_L$, with pitch, for both models. The two top plots are for the air-flight body; the bottom ones for water-flight. The plots in the left column are variations of $C_C$ with yaw; those on the right, the variations of $C_L$ with pitch. The $C_C$ yaw curves are averages of the plus and minus angle value; should be read plus for plus angles and minus for minus angles. Variations from the average, due to unintentional asymmetries, amounted to approximately $\pm$ 3 per cent and are an indication of the larger variations which might be expected in production from such a cause. The variation of the lift coefficient with plus or minus pitch was to have been expected from the horizontal design asymmetry. It may be noted that the difference caused by the nose and lug zone in the water-flight model (lower right) is reversed by the fins of the air-flight model (upper right). The solid, up-pitch lines are in their proper quadrant, both angles and values being positive. The dash lines have been transferred from the third quadrant to facilitate comparison; the angles and values should be taken as negative. All values shown in this figure are also affected by the aft support points. It is estimated from previous tests that the values shown are about 4-1/2 per cent and 9 per cent higher for the air- and water-flight models, respectively, than would have been obtained with support at the center of gravity.

Figure 6 shows the variation of the moment coefficient, $C_M$, (about the center of gravity) for both models when they yaw or pitch. The yaw curves are for C degree and 18C degree index, that is, normal position and upside down. They, also, are averages for plus and minus yaw with a $\pm$ variation of 2 per cent for the water-flight and 5 per cent for the air-flight model, due to unintentional asymmetry. It is readily apparent that the air-flight model is statically stable with yaw or pitch changes, while the water-flight model is statically unstable under such conditions. Although the values shown have been referred to the center of gravity, it is estimated from indications of previous tests that the $C_M$ values obtained with the aft support points are probably 2 per cent and 1C per cent low for the air- and water-flight models, respectively.

Figure 7 shows the effect of Reynolds number on the drag coefficient for noncavitating conditions over the water tunnel velocity range of 1C-65 feet per second for the air-flight model and 1C-6C feet per second for the water-flight model. The air velocity indicated, 6CC knots, is approximately 1CCC feet per second and gives a Reynolds number of about 49,CCC,CCC for the full scale projectile in atmospheric pressure and a temperature of 6C degree F. The extrapolated value of $C_D$ at this number is about C.165 but is not considered to be reliable as air compressibility enters as a vitiating factor at velocities so close to the speed of sound. The water-flight drag curve values also will not apply while the projectile is in that portion of its run where cavitation prevails.

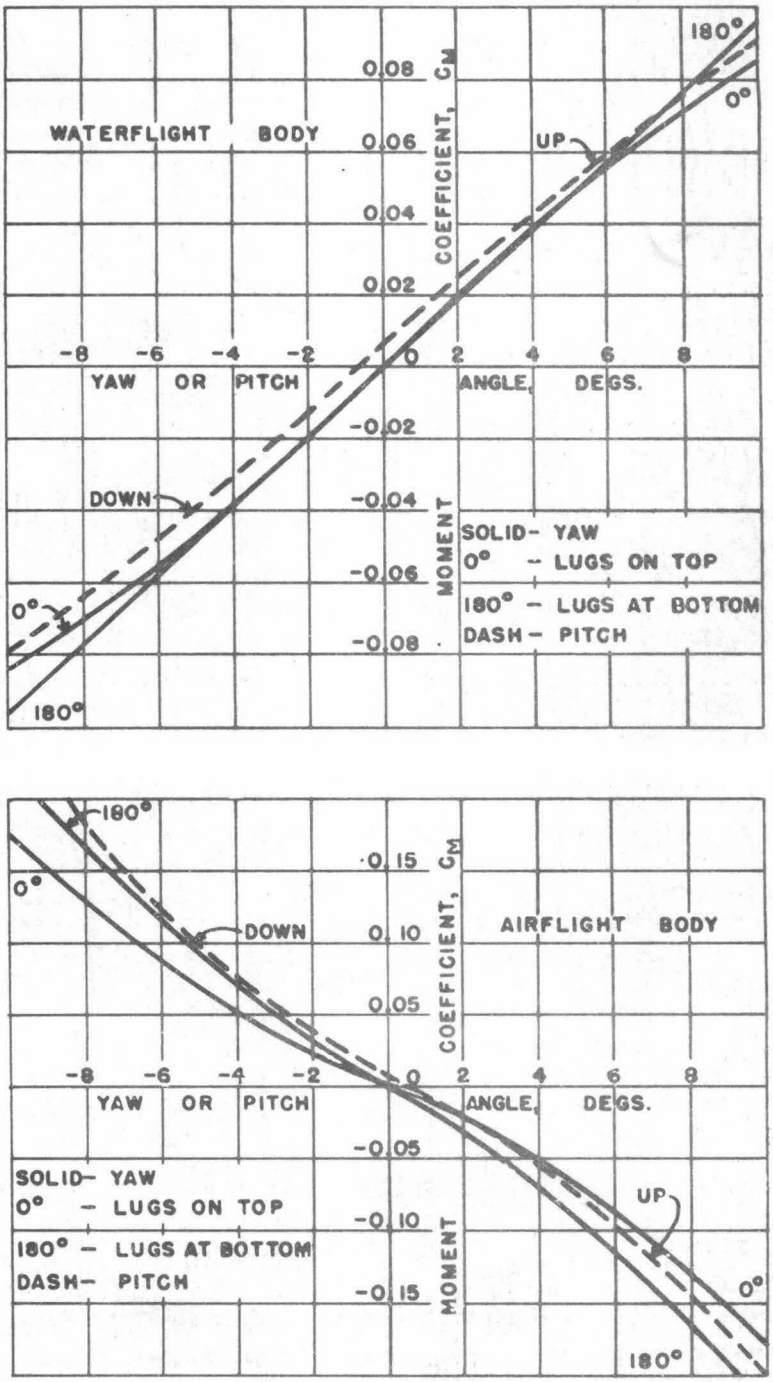


FIG. 6 — INFLUENCE OF YAW AND PITCH ANGLES ON MOMENT COEFFICIENT FOR 500 LB T16 S.P. BOMB

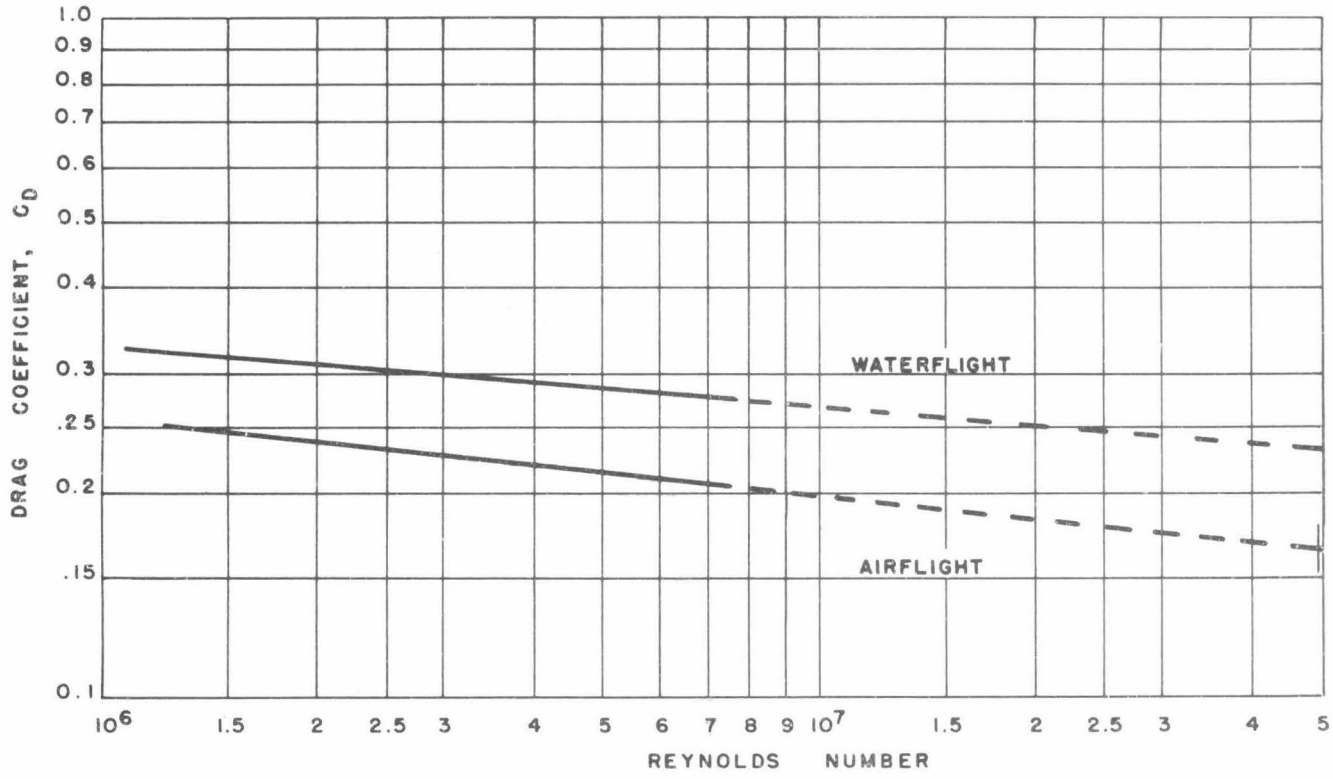


FIG. 7 — INFLUENCE OF REYNOLDS NUMBER ON DRAG COEFFICIENT OF 500 LB T16 S.P. BOMB UNDER NONCAVITATING CONDITIONS

Steady Incipient Cavitation

Cavitation conditions are generally referred to a cavitation parameter, K, a dimensionless number obtained from the formula

$$K = \frac{P_L - P_V}{1/2\ \rho V^2}$$

where

$P_L$ = absolute pressure of the fluid, lbs/sq ft

$P_V$ = vapor pressure of the fluid, lbs/sq ft

$\rho$ = mass density of fluid, weight in lbs/sq ft divided by acceleration of gravity

V = velocity of projectile in ft/sec

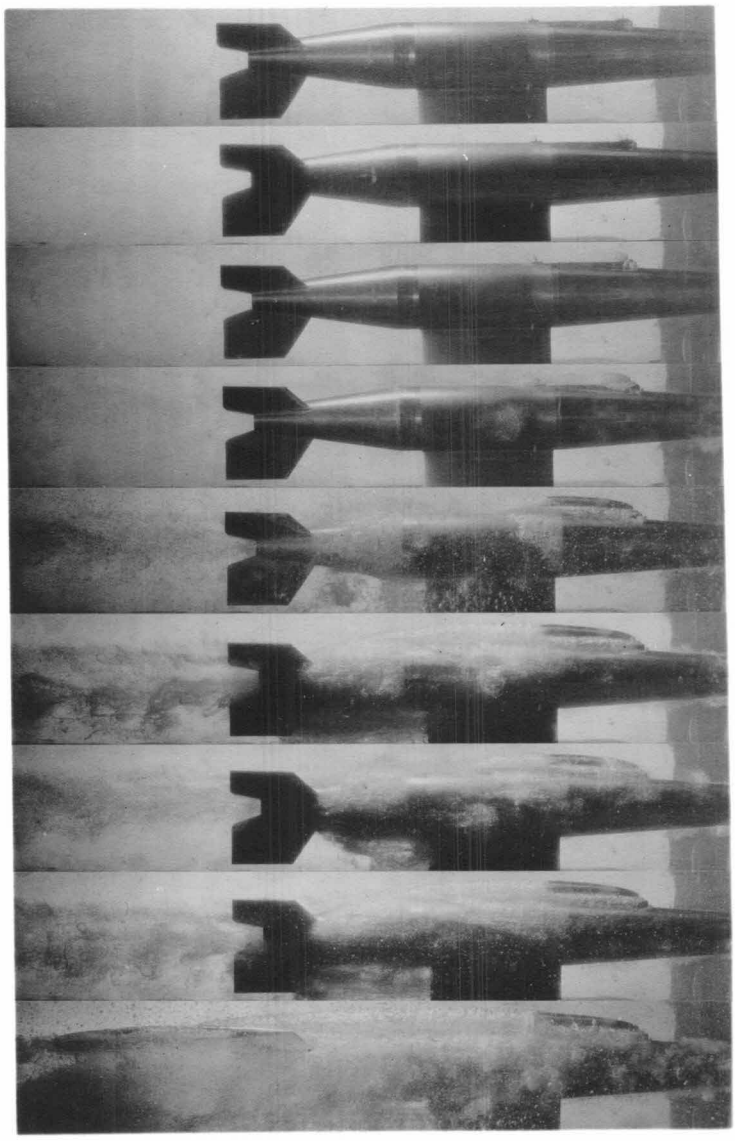


FIG. 8 – DEVELOPMENT OF CAVITATION ON AIR-FLIGHT MODEL OF 500 LB T16 S.P. BOMB
STRAIGHT SIDE VIEWS, NOSE OBSCURED

Steady incipient cavitation was established at the locations indicated and at K values as follows:

| Location | K |
|---|---|
| Forward Lug | 2.09 |
| Forward edge lug support | 1.92 |
| After lug | 1.65 |
| Nose | 1.41 |
| Leading edge of fins | 1.02 |
| Tail struts (water-flight) | 0.81 |
| Junction of afterbody and straight section | 0.56 |
| Junction of nose and straight section | 0.54 |

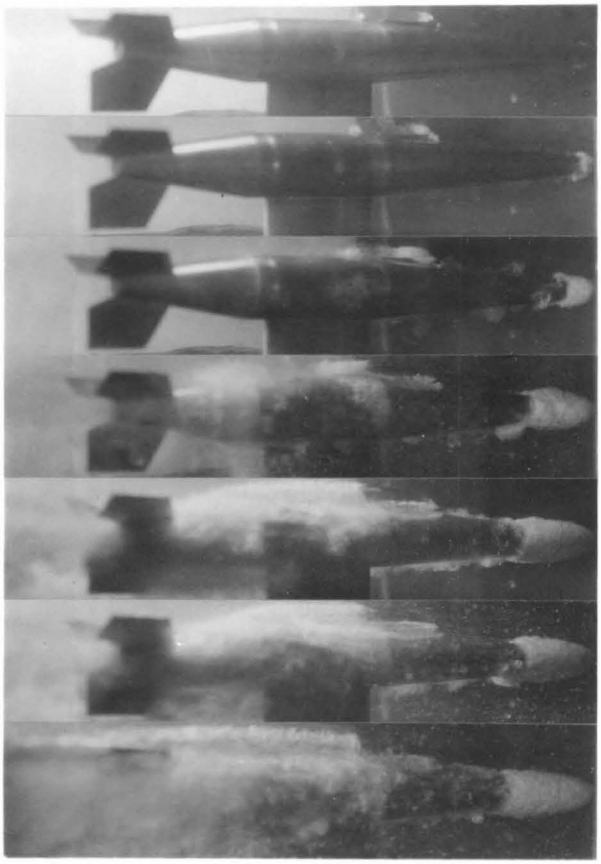


FIG. 9 – DEVELOPMENT OF CAVITATION ON AIR-FLIGHT MODEL OF 500 LB T16 S.P. BOMB
ANGLE VIEWS FROM SIDE SHOWING NOSE CAVITATION

The relatively great nose length of this model caused the nose tip to lie beyond the working section window and hence standard, straight side-view photographs did not show the collar of bubbles which formed. Angle shots from the side were, therefore, taken for this purpose and the straight side views are presented to show other cavitation in undistorted form. No top views are given as the top-view camera was used for the angle shots of the nose.

Figure 8 shows the customary straight side views of the air-flight model, and Figure 9, the nose photographs of the same model. Pictures in the two series may be correlated by the K values indicated. Some pictures have been omitted where nothing showed except the model or where there were no appreciable differences. Two pictures for K = 0.21 have been included in Figure 8 to show the amount of variation incident to attempts to obtain equal K values. Very small changes in settings have appreciable effects at such low K values. In the top photograph of this figure, K = 1.43, cavitation is present in both lugs and lug support, but very slight on the rear lug. The occurrence of steady incipient

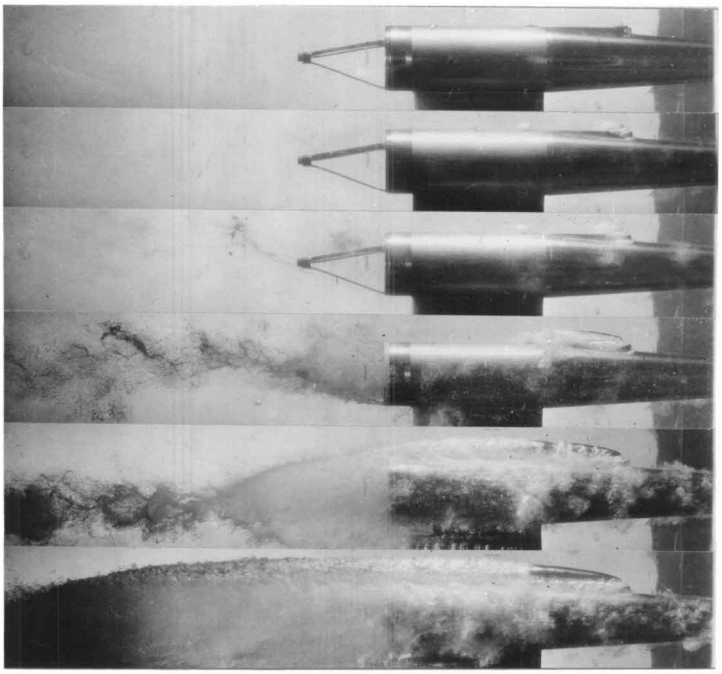


FIG. 10 — DEVELOPMENT OF CAVITATION ON WATER-FLIGHT MODEL OF 500 LB T16 S.P. BOMB
STRAIGHT SIDE VIEWS, NOSE OBSCURED

cavitation can be established by eye considerably before it will show in photographs. In the top photograph of Figure 9, K = 1.18, the nose cavitation is visible in an early stage and the cavitation bubbles from the lugs and lug platform may be seen more readily, because of lighting conditions, than in the corresponding view of Figure 8. For K = 0.77 there is cavitation on the leading edge of the fins but it is more apparent at K = 0.44. For K = 0.44, cavitation bubbles may also be seen at the junction of the afterbody and the cylindrical section. Cavitation has begun on the aft edge of the fins at K = 0.23. The remaining pictures show further bubble development to the maximum obtained. The present limitations of the High Speed Water Tunnel prevented, for this projectile, the development of the full bubble which was desired.

Figures 10 and 11 are similar series for the water-flight model, the former being the straight side views, with the latter showing the nose tip as well. The views for K = 1.83 and 1.21 were omitted from Figure 10 since no cavitation was visible with the light conditions existing. Some cavitation bubbles are visible for K = 1.83 (Figure 11) on the forward lug. The aft lug is not cavitating, the light area being due to reflections from the metal. For K = 1.21, both lugs, the lug support, and the nose show cavitation bubbles. It is slightly more advanced in the pictures for K = 1.19. Strut cavitation, hardly visible, has begun for K = 0.58. For K = 0.51, cavitation has started on the cylindrical part of the afterbody. The remaining views show further development to the maximum obtained.

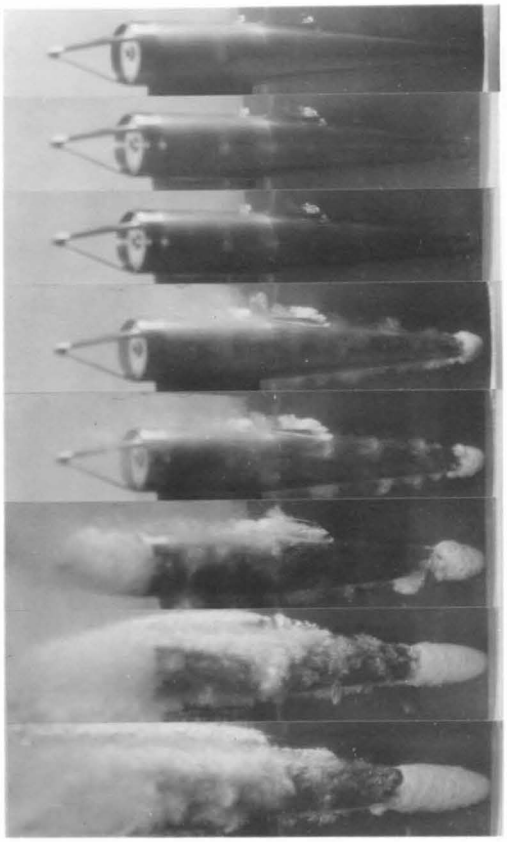


FIG. 11 – DEVELOPMENT OF CAVITATION ON WATER–FLIGHT MODEL OF 500 LB T16 S.P. BOMB
ANGLE VIEWS FROM SIDE SHOWING NOSE CAVITATION

Force Coefficients with Cavitation

It was desired to obtain force coefficients under conditions of full bubble cavitation. As stated above, a full cavitation bubble could not be obtained for this nose with present High Speed Water Tunnel limitations. Measurements were made for the water-flight model with a velocity of 50 feet per second and a K of 0.30 which gave a collar about two inches wide aft of the nose tip, a well developed stream from the lugs and lug support, and a blanket covering the upper diagonal half of the cylindrical portion (as viewed from the side) and coming from the junction of nose and cylindrical sections. There was, of course, also cavitation from the support shield. No attempt was made to correct for support interference owing to the conditions encountered. Consequently, the results shown in Figure 12 are not corrected for shield effects. Such corrections would be expected to reduce, somewhat, the values shown for all curves. Comparison with other tests for a nose of this type in full bubble, further indicates

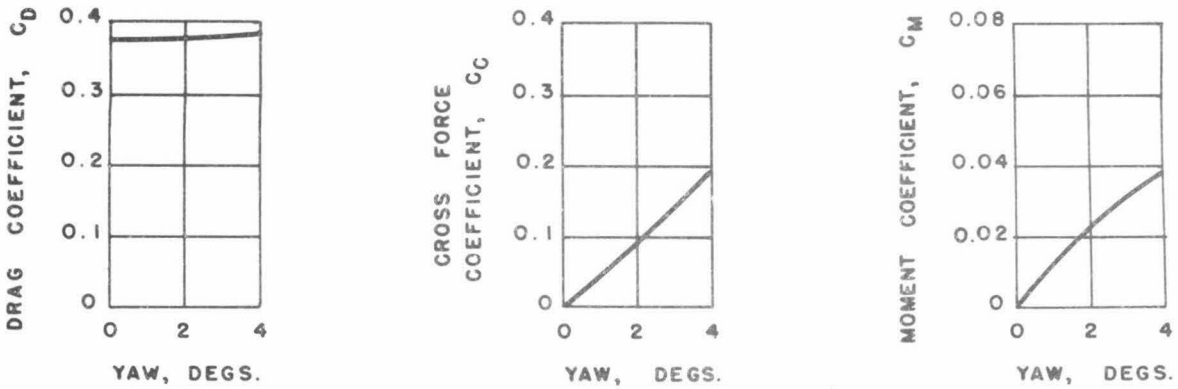


FIG. 12 – INFLUENCE OF YAW ANGLE ON FORCE COEFFICIENTS OF 500 LB T16 S.P. BOMB WITH WATER-FLIGHT AFTERBODY DURING CAVITATION VELOCITY 50 FT/SEC; K = 0.30

Note: This was not full bubble cavitation since it was impcssible to attain it for this nose with existing facilities

that when the data were obtained, full bubble had not been reached. It will be noted that in the bubble, the water-flight model is still statically unstable but it is less so than for noncavitating conditions. For cavitating conditions the cross force coefficient is also greater than without cavitation.

## FLOW LINE DRAWINGS

Figures 13, 14 and 15 are flow line drawings made from flow conditions observed in the Polarized Light Flume with the models of this projectile.

Figure 13 shows the air-flight model in profile, normal ($0^o$) index with zero and 10 degree "up" pitch. Eddy zones may be noted about the nose, lugs, and at the aft end of the afterbody. The size of the eddy zone is an indication of energy loss which contributes to the drag.

Figure 14 is the same model viewed from above for zero, and plus 10 degrees of yaw. Flow lines which were essentially unchanged from Figure 13 have not been repeated in order to emphasize the changes observed. There was, for instance, no appreciable difference in afterbody end disturbances.

Figure 15 shows the water-flight afterbody eddy zone. The structural pieces, even at 10 degrees, seem to lie in the zone of stagnant fluid and not in the high velocity flow. This tends to keep the drag coefficient lower than if such parts met the higher flow velocities. The higher drag coefficient of the water-flight model may thus be seen to be due primarily to the larger eddy zone following its blunt afterbody.

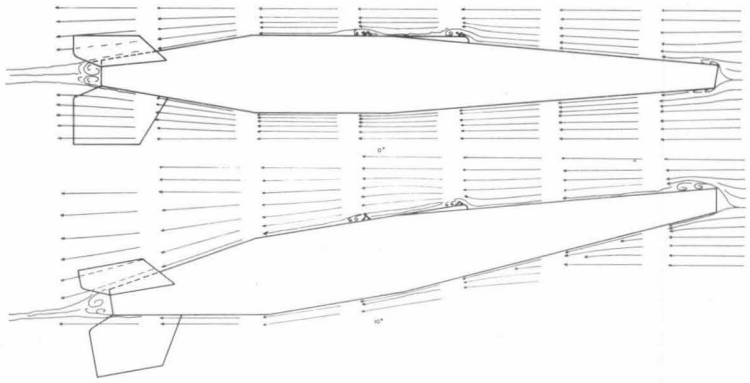

FIG. 13 – FLOW LINE DRAWINGS FOR 500 LB T16 S.P. BOMB

INDICES AT 0°

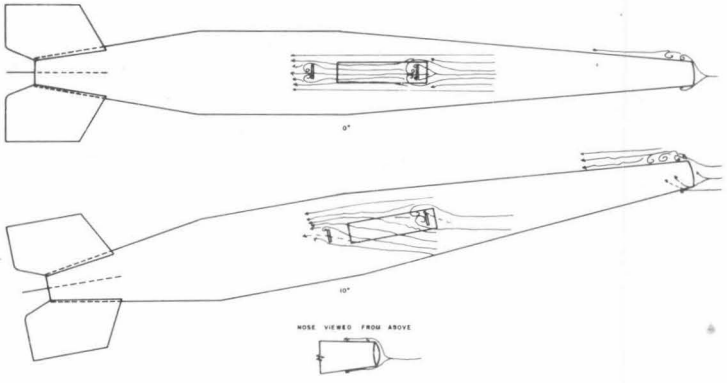


FIG. 14 – FLOW LINE DRAWINGS FOR 500 LB T16 S.P. BOMB

INDICES AT 10°

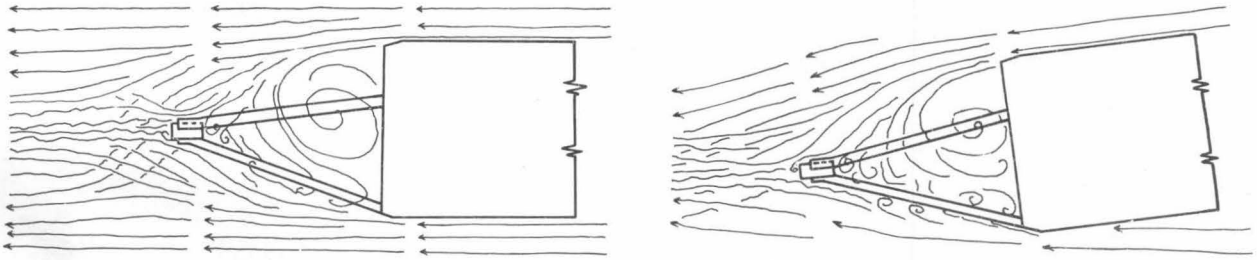

0° YAW 10° YAW

FIG. 15 – FLOW LINE DRAWINGS OF WATER–FLIGHT MODEL
AFTERBODY EDDY ZONE
500 LB T16 S.P. BOMB